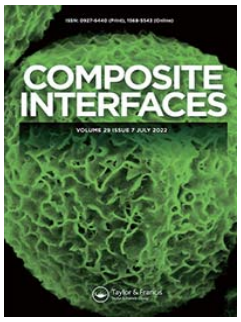

Composite Interfaces

ISSN: (Print) (Online) Journal homepage: https://www.tandfonline.com/loi/tcoi20

Interfacial adhesion evaluation *via* wettability for fiber reinforced polymer composites: A review

Jong-Hyun Kim, Dong-Jun Kwon, Choong-Sun Lim, Bong-Kuk Seo, K. Lawrence DeVries & Joung-Man Park

To cite this article: Jong-Hyun Kim, Dong-Jun Kwon, Choong-Sun Lim, Bong-Kuk Seo, K. Lawrence DeVries & Joung-Man Park (2022): Interfacial adhesion evaluation *via* wettability for fiber reinforced polymer composites: A review, Composite Interfaces, DOI: 10.1080/09276440.2022.2099519

To link to this article: https://doi.org/10.1080/09276440.2022.2099519

Published online: 11 Jul 2022.

COMPOSITE INTERFACES
https://doi.org/10.1080/09276440.2022.2099519

Taylor & Francis
Taylor & Francis Group

REVIEW ARTICLE

Interfacial adhesion evaluation *via* wettability for fiber reinforced polymer composites: A review

Jong-Hyun Kim[a], Dong-Jun Kwon[b], Choong-Sun Lim[a], Bong-Kuk Seo[a], K. Lawrence DeVries[c] and Joung-Man Park[b,c,d]

[a]Center for Advanced Specialty Chemicals, Korea Research Institute of Chemical Technology, Ulsan, Republic of Korea; [b]Department of Materials Engineering and Convergence Technology, Gyeongsang National University, Jinju, Republic of Korea; [c]Department of Mechanical Engineering, The University of Utah, Salt Lake City, Utah, USA; [d]Research Institute for Green Energy Convergence Technology, Gyeongsang National University, Jinju, Republic of Korea

ABSTRACT

As the demand for fiber-reinforced composite (FRC) has increased in various industries, composite materials have been manufactured in larger sizes and more complex shapes. Since the FRC has been manufactured in such larger and more complex shapes, wettability, one of the important factors in FRC manufacturing efficiency, has been the focus of many researchers. This paper explores various evaluation methods of the wettability between fiber and polymer matrix. Generally, work of adhesion, capillary, and permeability methods have been used to evaluate the wettability parameters between the fibers and the polymer matrix. These three parameters exhibit different scales of measurements such as surface energy, viscosity of the polymer, the fiber volume fraction, fiber orientation, and so on. Future research may include complementary studies between these evaluation methods.

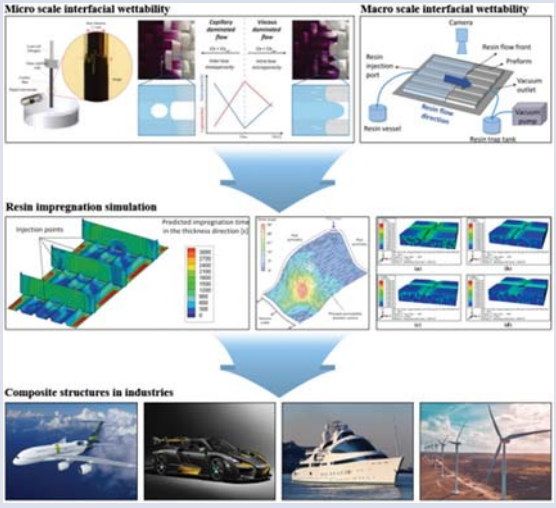

ARTICLE HISTORY
Received 1 July 2022
Accepted 1 July 2022

KEYWORDS
Fiber-reinforced composite (FRC); evaluation methods of wettability; work of adhesion; capillary; permeability

Bong-Kuk Seo bksea@krict.re.krCenter for Advanced Specialty Chemicals Korea Research Institute of Chemical Technology, Ulsan, Republic of Korea; CONTACT Joung-Man Park jmpark@gnu.ac.kr Department of Materials Engineering and Convergence Technology, Gyeongsang National University, Jinju 52828, Republic of Korea

1. Introduction

1.1. The importance of wettability in fiber-reinforced composite

Due to their lightweight and good mechanical properties, application of fiber-reinforced composites (FRC) has been tried as structural materials in many industries [1,2]. FRC materials have been developed and used for a wide range of applications in aircraft, ships, automobiles, wind turbine blades, and so on [3,4]. As the demand for FRC has increased in various industries, FRC materials are being manufactured more quickly and elaborately with near-zero defect rates [5,6]. Wettability is one factor used to evaluate manufacturing efficiency, and interfacial properties can be evaluated by this factor in a roundabout way [7–9].

To improve the manufacturing efficiency of composite materials, the wettability, between fiber and polymer resin, should be improved. In the case of poor wettability, the polymer matrix does not fully impregnate the fibers [10–12]. This can lead to micro voids, dry zones, and poor reinforcement [13,14]. Poor wettability also led to low mechanical properties of FRC due to poor interfacial properties. Load transfer from fiber reinforcement to polymer matrix is dominated by the interface between fiber and matrix. Good interfacial properties reduce local stress concentrations and internal crack propagation thereby increasing the mechanical performance of the composite [15–17].

The wettability between fiber and polymer matrix has been evaluated using various evaluation methods. In general, work of adhesion [18–20], capillary action [21–23], and permeability [24–26] are used to evaluate wettability, under different material conditions, to optimize the manufacturing efficiency of the FRC. Three parameters were calculated under different material conditions, and previous publications have studied how modifying the equations of wettability with these different conditions can improve wettability.

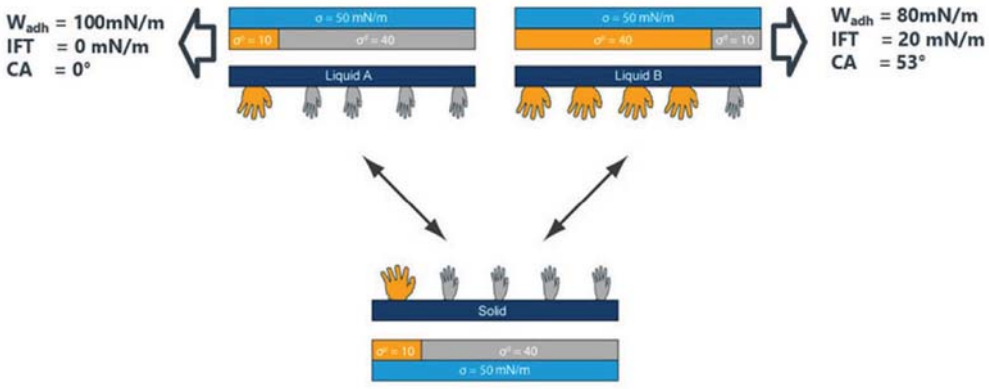

Figure 1. Schematic arrangement of work of adhesion with polar and disperse components [27].

2. Experimental

2.1. Surface energies and work of adhesion

Surface energy and work of adhesion have been used to predict wettability between two different materials. Figure 1 shows two liquids with the same surface tension but opposite polar and disperse component ratios. The polar and disperse components of both the liquid and substrate are designated as the yellow and gray bands, respectively. When the liquid and solid come into contact, the liquid and the substrate with the highest interaction (liquid A) show the highest work of adhesion and the lowest interfacial tension. This suggests that liquid A and substrate combination will have a better initial adhesion and, over time, will be more stable than liquid B. Liquid B has a minimal interaction with the substrate, lower work of adhesion and higher interfacial tension [27–29].

In FRC, the wettability between fiber and polymer resin was determined using the work of adhesion, W_a. The contact angles (CA) of fiber and polymer resin were measured using four different solvents (i.e., distilled water, formamide, ethylene glycol, and diiodomethane) for static and dynamic CAs. The contact angles were calculated using Young's equation [30]:

$$\gamma_S - \gamma_{SL} = \gamma_L \cos\theta \tag{1}$$

where γ_L, γ_{SL}, and γ_S are the liquid surface tension, the solid/liquid interfacial energy, and the solid surface energy, respectively. The total surface energy, γ^T, is the sum of the Lifshitz-van der Waals component, γ^{LW} and the acid-base component, γ^{AB}. The calculation of these components followed the modified young-Dupre equation [31] of the work of adhesion, W_a expressed as:

$$W_a = \gamma_L(1+\cos\theta) = 2\left(\gamma_L^{LW}\gamma_S^{LW}\right)^{\frac{1}{2}} + 2\left[\left(\gamma_S^-\gamma_L^+\right)^{\frac{1}{2}} + \left(\gamma_S^+\gamma_L^-\right)^{\frac{1}{2}}\right] \tag{2}$$

A commonly used approach, in considering solid surface energies, is to express them as the sum of dispersive and polar components which influences the work of adhesion, W_a, between the surface of the reinforcement material and the matrix. To determine the polar and dispersive surface free energies, the Owens–Wendt equation [32] is used, expressed as:

$$W_a = \gamma_L(1+\cos\theta) = 2\left(\gamma_S^d\gamma_L^d\right)^{\frac{1}{2}} + 2\left(\gamma_S^p\gamma_L^p\right)^{\frac{1}{2}} \tag{3}$$

where γ_L, γ_L^d, and γ_L^p are known for the testing liquids and γ_S^p and γ_S^d can be calculated from the measured contact angles. Based on the surface energy of the material, the work of adhesion between the fiber and polymer resin was obtained predicting an improvement in interfacial adhesion [33–35].

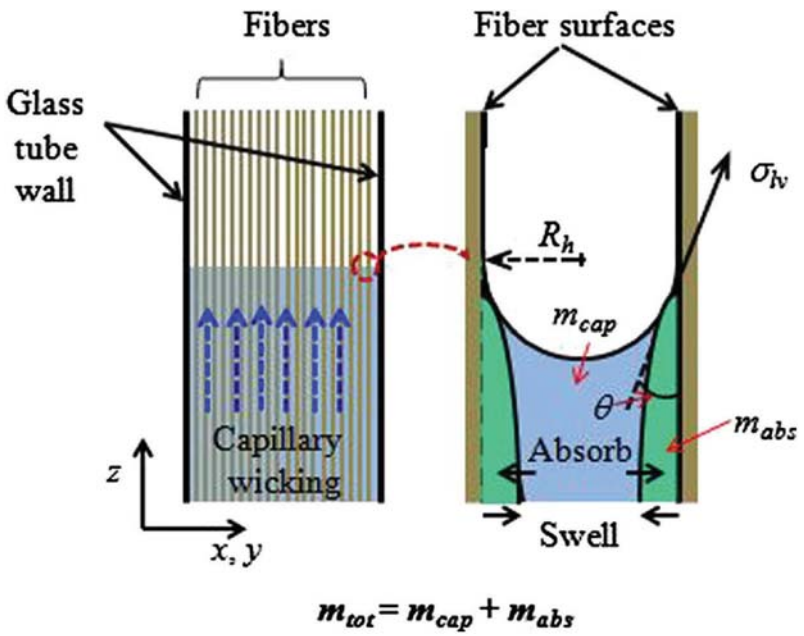

Figure 2. Schematic arrangement of the capillary test [21].

2.2. Capillary

Capillary action is defined as the movement of fluid within the spaces of a porous material due to the intermolecular forces between the liquid and the surrounding solid surfaces that enable the liquid to flow into narrow spaces without the assistance of, or even in opposition to, external forces like gravity [36–38]. In composite materials, this action can be shown by resin impregnation on a micro scale.

In Figure 2, a capillary test method was suggested, using a schematic arrangement. A glass capillary tube with a fiber tow just touched the surface of the polymer causing the resin to impregnate the fiber tow. The variation in weight of the specimens was measured

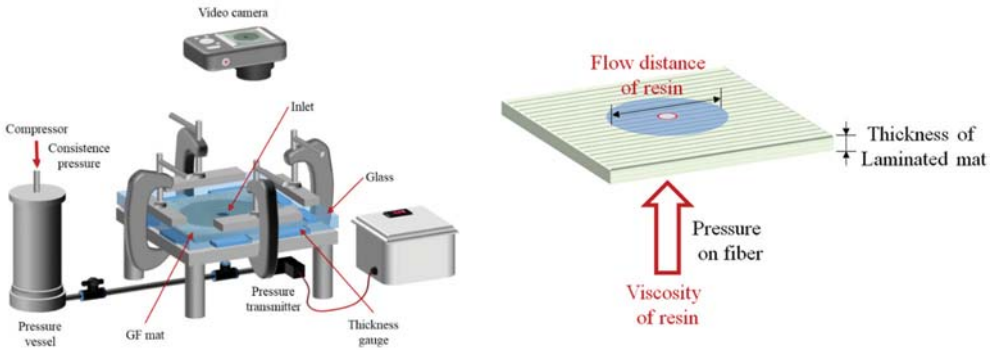

Figure 3. Schematic arrangement for permeability measurement of fiber mat by the polymer resin [24].

and the experimental height of resin impregnation was observed in situ, using a USB microscope. The height of resin impregnation was compared with the calculated height, using Washburn's equation [39]:

$$h^2(t) = \left\{\frac{(cr)}{2}\right\}\frac{\gamma_L \cos\theta_a}{\eta}t \tag{4}$$

where h is the height of resin impregnation, t is the time, and c is a parameter considering tortuosity. r is the mean porous radius, θ_a is the apparent advancing CA, γ_L is the liquid surface tension of the epoxy resin, and η is the viscosity of the resin.

2.3. Permeability

For FRC, permeability is the resin impregnation factor into a fiber mat on a macro scale. It is a key parameter in liquid composite molding processes; it is a well-defined concept, but still a difficult parameter to quantify, in large part because textile reinforcements are not constant in their internal geometry [40,41]. Permeability is affected by the density and surface area of reinforcing material, the viscosity of the resin, the design of the mold, and so on. A schematic plot of this permeability measurement is shown in Figure 3 and equation (5) relates permeability to the various resin and mat parameters [42]:

$$K_f = -q_f\frac{\mu \cdot h_f}{P_f} \tag{5}$$

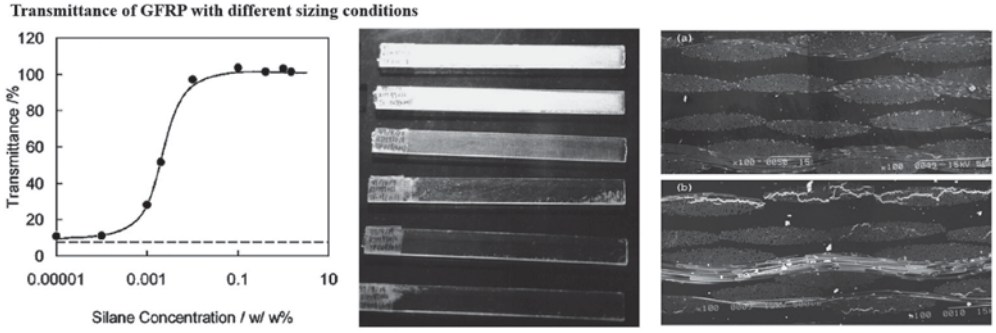

Relative surface tension of materials

Liquid medium	Water	Ethylene glycol	UP (r. m.)	UP (100°C)
Relative surface tension*	0.43	0.80	0.97	0.92

*(Surface Tension of Silane-treated Glass Cloth)/(Surface Tension of Untreated Glass Cloth).

Figure 4. Transmittance of GFRP and relative surface tension of materials with different silane concentrations [12].

where, K_f is the permeability of the fiber mat, q_f is the flow distance of the resin into the fiber mat, μ is the viscosity of the resin, h_f is the thickness of the laminated FRC and P_f is the pressure on the fiber mat. The fiber volume fraction (FVF) was determined using equation (6) and was kept constant for all the permeability measurements.

$$FVF = \frac{FAW \cdot N_f}{\rho_f \cdot \ h_f} \tag{6}$$

where FAW is fiber area weight, N_f is number layers in the fabric mats, ρ_f is the density of the fiber, and h_f is the thickness of the FRC.

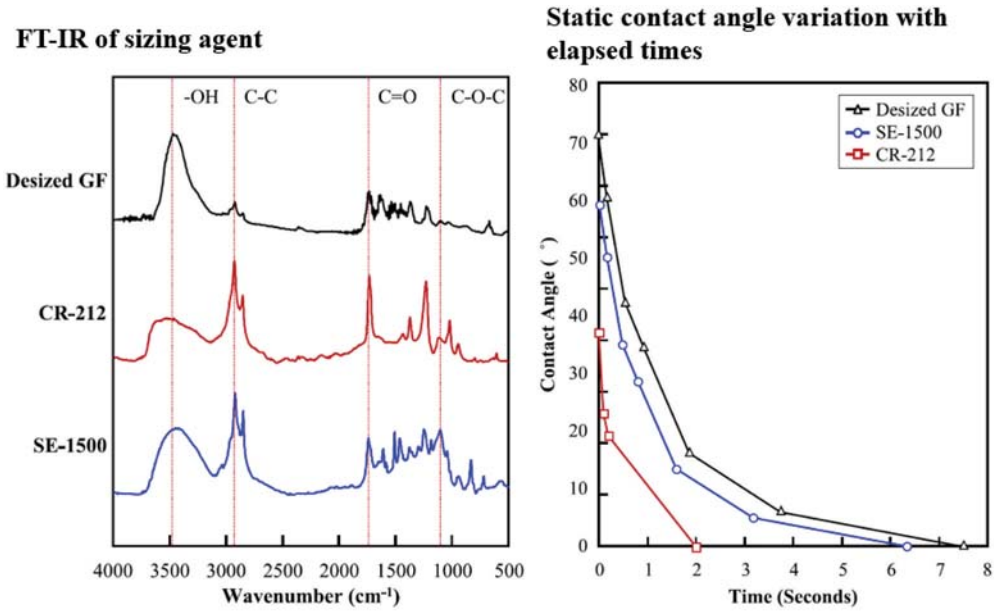

Surface energies and work of adhesion of materials

	γ_s	γ_s^{LW}	γ_s^{AB}	γ_s^{+}	γ_s^{-}	γ^d	γ^p	W_a
DCPD	24.9	19.6	5.2	17.8	0.4	10.1	8.6	–
Desized GF	32.6	25.8	6.9	36.6	0.3	12.0	29.3	57.3
SE-1500	34.2	25.5	8.7	22.1	0.8	15.5	21.0	58.4
CR-212	38.1	35.4	2.7	4.2	0.4	32.4	4.6	60.8

Figure 5. Surface energy and work of adhesion between glass fiber and *p*-DCPD for different sizing agent treatments [46].

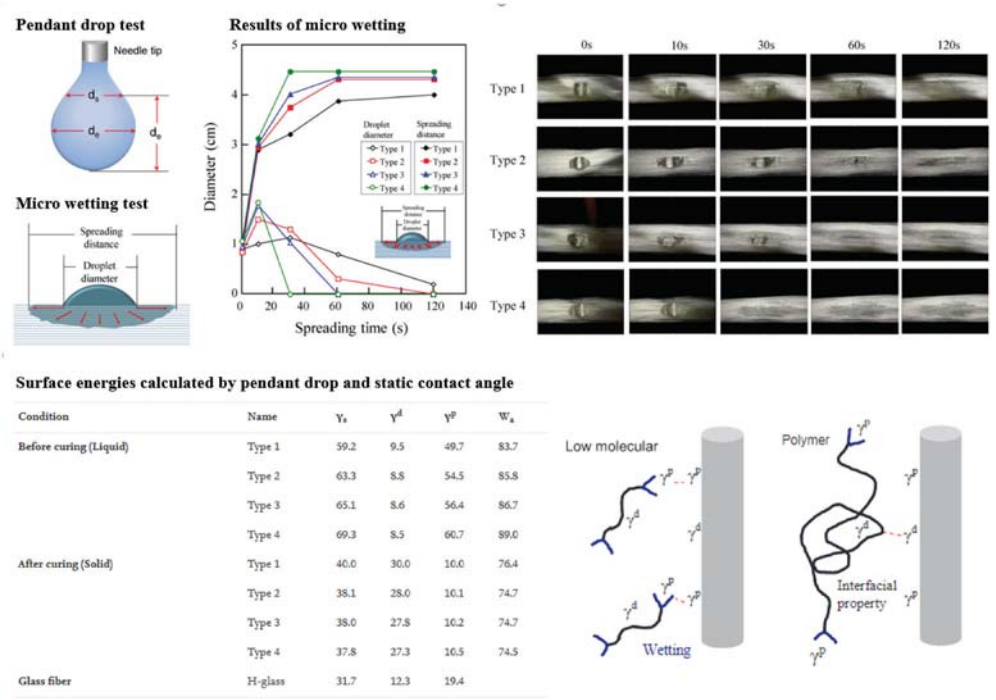

Figure 6. Surface energy and work of adhesion between glass fiber and epoxy resin with different epoxy resin formulations and curing state [51].

3. Research trend of wettability in fiber-reinforced composites

3.1. Evaluation of wettability using surface energies and work of adhesion

The surface energies and work of adhesion between fiber and polymer matrix are defined as the reversible thermodynamic work required to separate the interface from the equilibrium state of two phases to an infinite separation distance [43–45]. The determination of these parameters is one of the classical evaluation methods for wettability in thermodynamic aspects. The research of Ohnishi *et al.* [12] focused on the wettability between glass fiber (GF) and unsaturated polyester (UP) with different silane concentrations using transmittance of composite and relative surface tension between GF and UP. As shown in Figure 4, the transmittance of the composite was improved as the silane concentration increased to 0.1 wt%. In the FE-SEM photos, the UP resin could not be impregnated well into GF in the case of low silane concentration. The light, which was passed through the composite, was scattered by voids, and the transmittance was reduced. The wettability between GF and UP was evaluated using relative surface tension. As the silane was treated on the GF surface, the relative surface tension exhibited below 1 in all of the solvent and UP resin cases as shown in the summarized table. Using this table, the wettability of UP resin was improved as the silane treatment on GF surface.

Mechanical properties of fiber reinforced composite with different resin conditions

Type of resin	Tensile property		Impact strength (KJ/m^2)	Flexural modulus (GPa)
	Tensile strength (MPa)	Elongation at break (%)		
Original VR	81.95	5.34	2.68	3.37
LNBR/VR	59.47	6.89	4.22	3.08
PIB/VR	53.37	6.56	5.13	3.02
I-HTPB/VR	47.38	7.05	3.60	2.16
I-TPO/VR	8.50	18.20	8.29	0.25

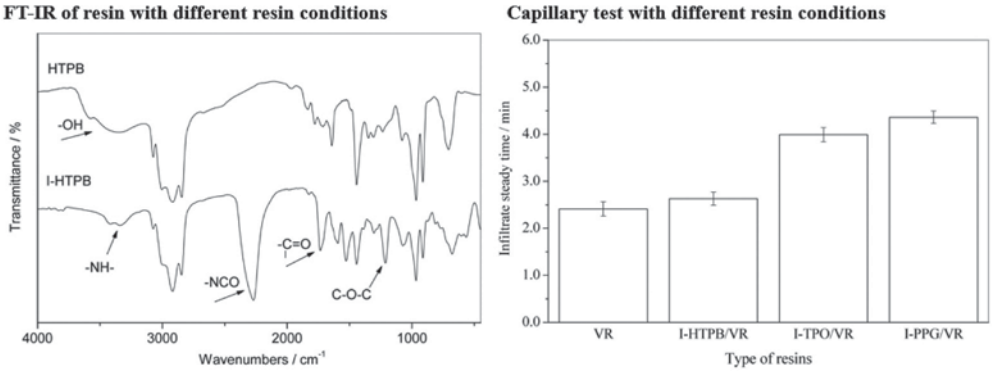

Figure 7. Surface energy and work of adhesion between glass fiber and epoxy resin with different epoxy resin formulations and curing state [58].

The research of J.H. Kim *et al.* [46] focused on the wettability between GF and *p*-dicyclopentadiene (*p*-DCPD) used surface energies and work of adhesion for different sizing agent conditions. As shown in Figure 5, as the dispersion component of surface energies increased, the work of adhesion also increased for different hydroxyl group amounts, indicated by FT-IR peaks. Static CA measurements were performed to determine the wettability compared to the work of adhesion. As the work of adhesion increased, the decreasing rate of static CA for *p*-DCPD was accelerated. This paper will demonstrate that the wettability of *p*-DCPD resin into GF, was improved as the hydroxyl group of sizing agent decreased [47,48].

Static and dynamic CA are usually used to calculate surface energies of fiber and polymer matrix in the solid state. In the case of the polymer matrix, however, some polymer matrixes, such as epoxy and unsaturated polyester, have been used in uncured states to impregnate the polymer resin into the fibers. In this state, surface energies might differ from those in the cured states [49,50]. To resolve this issue, Shin *et al.* [51] calculated the surface energies using the pendant drop test and compared the results with those of the micro wetting test for different epoxy formulations, with the results shown in Figure 6. The un-cured epoxy resins have a low molecular weight containing a number of functional groups. Functional groups pose the potential for polar interactions [52,53]. This led to a higher work of adhesion than that of cured epoxy. Long chains result in a more intermittent dispersive interaction [54,55]. This dispersive interaction produces bonding between the glass fiber and the epoxy resins as well as improved interfacial properties.

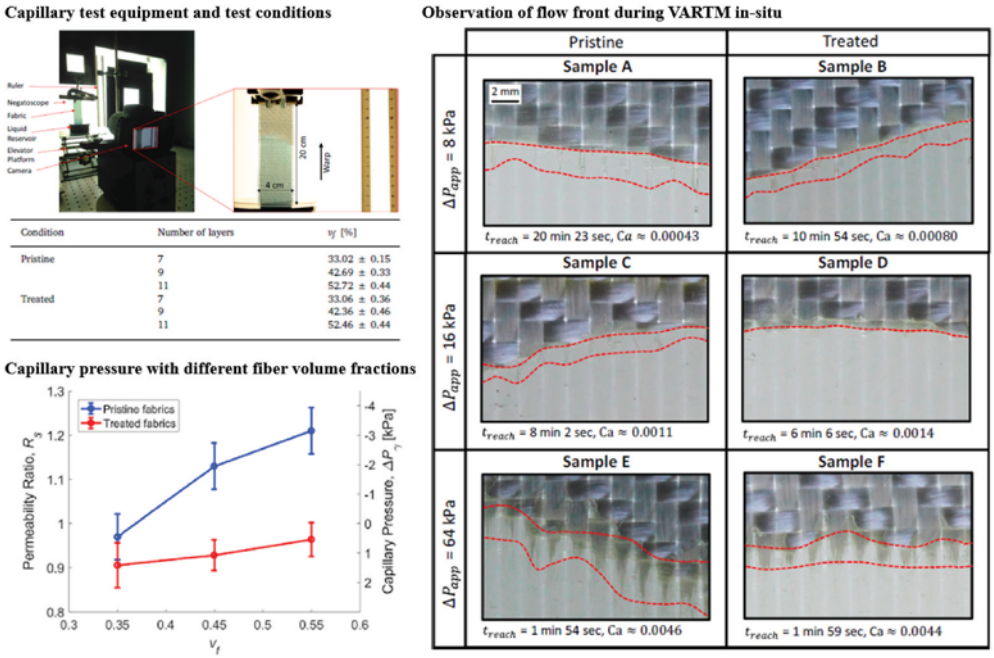

Figure 8. Capillary testing and flow front observation for different FVF and surface treatments [59].

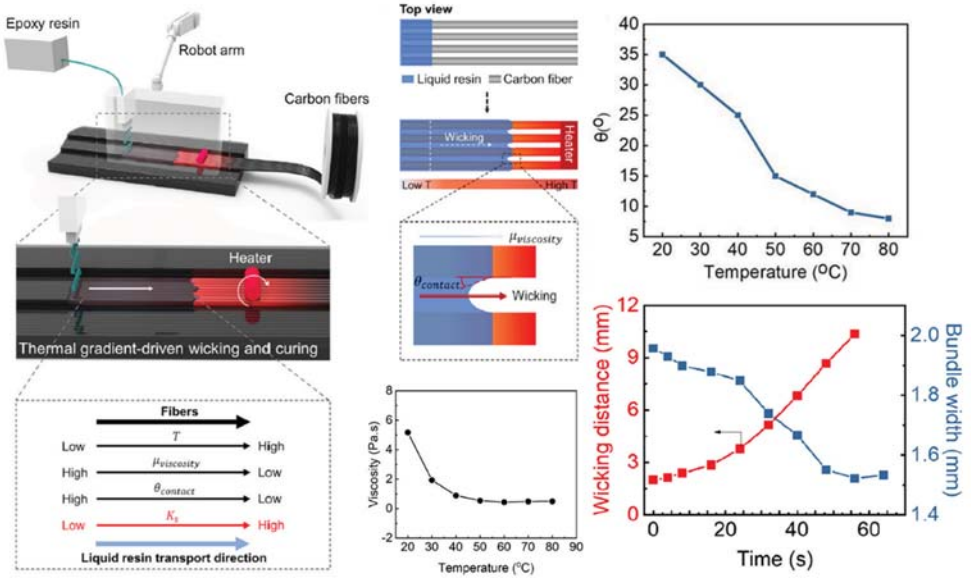

Figure 9. Capillary tests on carbon fibers and epoxy resin at different temperatures [65].

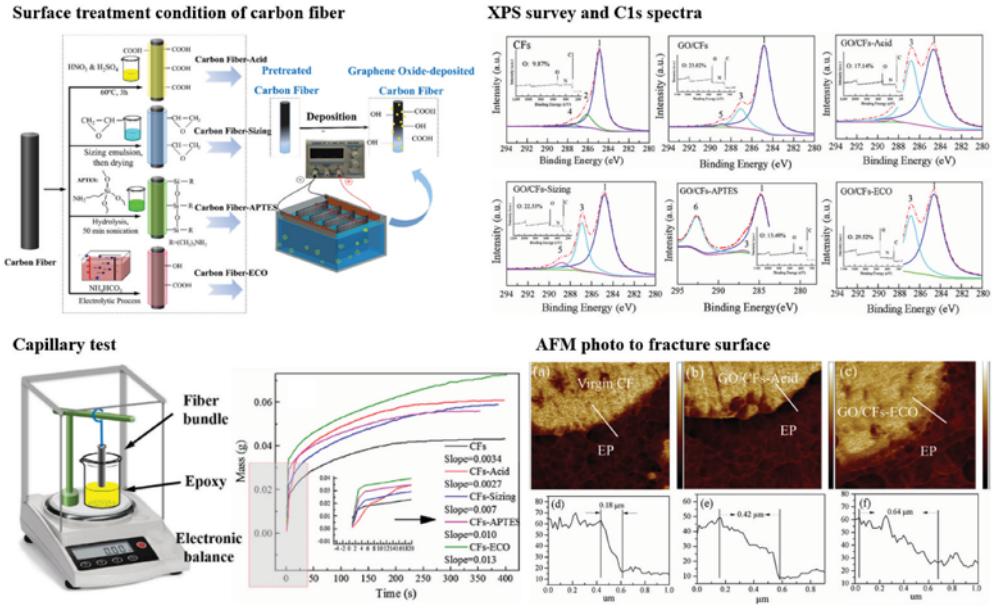

Figure 10. Capillary test and interface observation of carbon fiber and epoxy resin with different surface treatments [68].

3.2. Evaluation of wettability using capillary parameter

The capillary parameter is affected by material conditions and surface energies between fiber and polymer resin [56,57]. The capillary evaluation could be determined more quantitatively than the work of adhesion in micro-scale and material engineering aspects. The research of Zheng *et al.* [58] focused on the wetting behavior of vinylester resin (VR) into ultrahigh molecular weight polyester (UHMWPE) fiber with different resin conditions using capillary test. In this publication (Figure 7), many liquid rubbers were added to improve wettability such as liquid nitrile-butadiene rubber (LNBR), liquid polyisobutylene (PBR), hydroxyl-terminated liquid polybutadiene rubber (HTPB), and polyether triols (TPO). As the rubber materials were added into VR, the impact property was improved, while tensile strength decreased. To analyze chemical groups of VR, the FT-IR peak was determined, and there existed many functional groups in VR that could help to improve the wettability by hydrogen bonding such as the hydroxyl, cyano, and etc. As shown in capillary data, the wettability of VR was improved in the rubber materials added cases.

Caglar *et al.* [59] studied the capillary parameter contribution in fabrics with different fiber volume fractions and surface treatments. The fiber volume fraction is one of the main factors controlling the mechanical properties of FRC [60–62]. In Figure 8, as the fiber volume fraction increased, the impregnation of the polymer resin decreased, while the mechanical properties improved. As shown in the photos of the flow front, the resin flow front was moved further forward than the full-impregnation front as the fiber volume fraction decreased. In the resin transfer

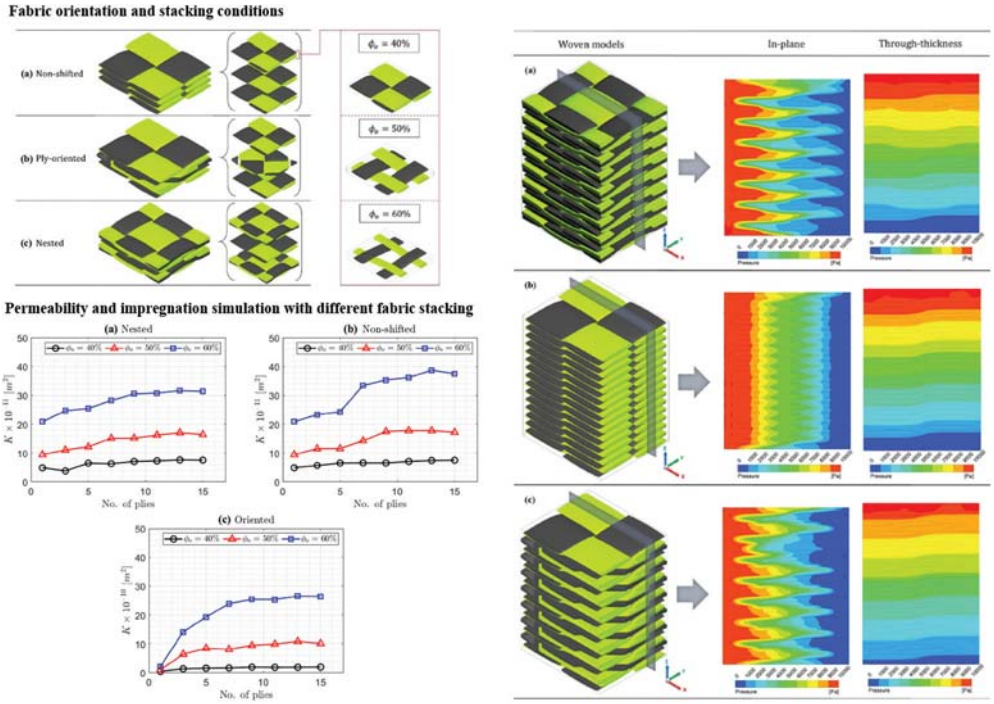

Figure 11. Permeability and impregnation simulation with different fabric orientations and stacking conditions [74].

molding (RTM) process, the resin flow progression is determined by the flow front, and it leads to a more stable and quicker resin flow. It may prevent micro-void formation in the composite and dry zone [63,64].

Figure 9 shows the results of research by B. Shi *et al.* [65] on carbon fiber reinforced epoxy composites, using the viscosity effects of the capillary parameter for 3D printer filaments. The viscosity of the epoxy resin was controlled using a Joule-Heater. As the temperature of the resin increased, as a result of increasing the carbon fiber temperature, the resin viscosity decreased dramatically. The contact angle in the meniscus also decreased as a result of the decreasing viscosity. This was influenced by the more active chain mobility, leading to improved work of adhesion between carbon fiber and resin and the improved impregnation of the resin into the carbon fibers [66,67].

The capillary parameter also influences the surface conditions of the fibers, and it is a factor affecting the contact angle in Darcy's law. Figure 10 shows research results of X. Yuan *et al.* [68] on the wettability of graphene oxide treated carbon fiber with different treatment methods. The surface was analyzed, and the elemental composition of oxygen was determined. Using the data from this analysis, the wettability of the fibers was determined. The wettability was evaluated using the capillary test, and the wettability was improved as the functional group content increased, which included oxygen. The fracture area was observed, using AFM analysis focused on the interface between the fiber and the epoxy matrix. The

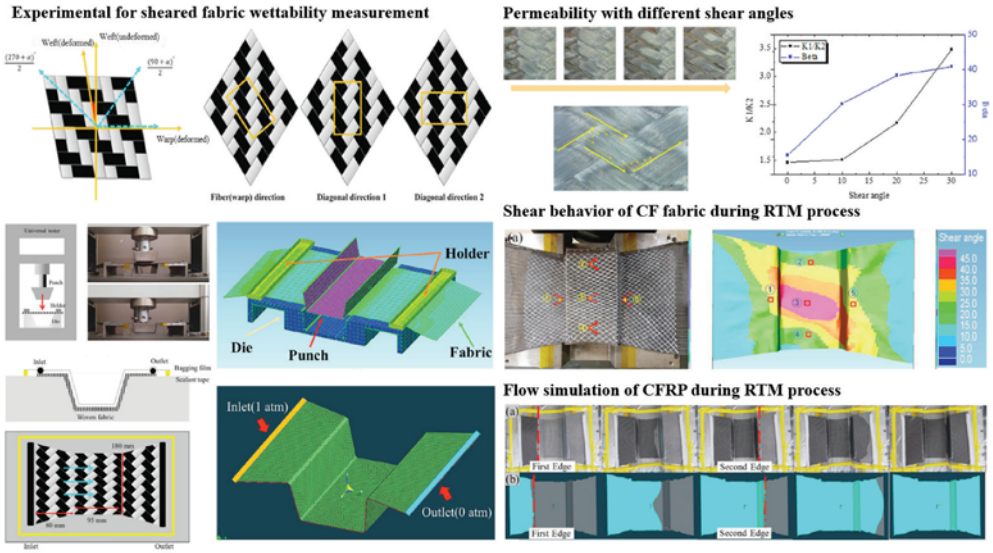

Figure 12. Permeability and impregnation simulation for carbon fibers and epoxy resin with different shear angles of carbon fabric [82].

surface roughness gradually decreased as the functional group content, which included oxygen, was increased. As shown in these results, the interfacial properties were also improved as the oxygen included functional group content increased [69,70].

3.3. Evaluation of wettability using permeability parameter

The permeability is affected by the bulk conditions of a material and manufacturing processing, and their parameters can be determined more quantitatively than work of adhesion in macro-scale in mechanical engineering aspects [71–73]. This parameter can be used for the simulation of resin impregnation for RTM process as well. Alotaibi *et al.* [74] investigated the permeability of fiber reinforced polymer composites with different fiber orientations and laminate stackings. Some of their results are shown in Figure 11. The flow behavior for in-plane and through-thickness was evaluated using permeability for different fiber orientations and laminate stackings. Using these data, the flow behaviors could be visualized using pressure gradient contours. As the fiber orientation became more complex, the flow of the resin in the through-thickness direction exhibited increased flow resistance, which could lead to void formation [75,76]. In this paper, it was found that an evaluation of the dual-scale void during the resin impregnation was important, and it needed to be predicted to prevent failures such as micro-voids and dry zone.

In the real RTM process, the fabric arrangement cannot be controlled homogeneously by shear in the curved edge [77–79]. Fabric arrangement affects resin flow due to the changing fiber volume fraction in specific areas [80,81]. Figure 12 shows results of some of the research of Kim *et al.* [82] in which the permeability of composites was calculated as the fabric was deformed by shear, and the resin flow in the RTM process for complex shapes was predicted with simulation applied with the shear parameter of fabric. The permeability was calculated

for different fabric shear angles, and the aspect ratio of permeability increased dynamically as the shear angle increased. This result was applied to a practical simulation system for resin flow prediction. In the punched section, the fabric was deformed dramatically due to shear behavior by tensile stress [83,84]. The flow during RTM was simulated based on permeability with different shear angles of fabric, and compared with the flow behavior of resin during real RTM processes. As shown in the figures, the resin flow was delayed in sections of deformed fabric. In the RTM process, The behavior of the resin flow front exhibited similarly compared with the simulation.

4. Conclusions

FRC is used in various industries to improve the body weight of structures. As the size and shape of FRC are bigger and more complex in these structural materials, it is important that we have knowledge of wettability in order to find the optimized manufacturing methods and efficiency for FRC. This paper summarizes, from previous publications, the current trends of evaluation methods for wettability, with different scales and material conditions. Micro-scale evaluation methods affect basic material conditions such as surface energies of fiber and polymer resin, formulation of resin, and so on. On a macro-scale, the bulk conditions to manufacture FRC are influenced by wettability such as fiber volume fractions, injection pressure, fabric orientation, and so on. In the future research, studies will be conducted on how these parameters complement each other, and how wettability might be improved to more efficiently and accurately manufacture larger and more complex FRC.

Disclosure statement

No potential conflict of interest was reported by the author(s).

Funding

This research was supported by KRICT core-project under Grant No. SS2241-10 and No. XI19-04; Basic Science Research Program through the National Research Foundation of Korea (NRF) funded by the Ministry of Education under Grant No. 2016R1D1A1B01012620 and No. 2020R1A6A1A03038697

ORCID

Jong-Hyun Kim http://orcid.org/0000-0002-1782-5442
Joung-Man Park http://orcid.org/0000-0002-6245-0758

References

[1] Valorosi F, Meo ED, Blanco-Varela T, et al. Graphene and related materials in hierarchical fiber composites: production techniques and key industrial benefits. Compos Sci Technol. 2020;185:107848.
[2] Kwon DJ, Kim NSR, Jang YJ, et al. Investigation of impact resistance performance of carbon fiber reinforced polypropylene composites with different lamination to applicate fender parts. Compos B Eng. 2021;215:108767.

[3] Sargianis J, Suhr J. Core material effect on wave number and vibrational damping characteristics in carbon fiber sandwich composites. Compos Sci Technol. 2012;72(13):1493–1499.
[4] Zhang J, Chevali VS, Wang H, et al. Current status of carbon fibre and carbon fibre composites recycling. Compos B Eng. 2020;193:108053.
[5] Rubino F, Nistico A, Tucci F, et al. Marine application of fiber reinforced composites: a review. J Mar Sci Eng. 2020;8(1):26.
[6] Li M, Pu Y, Thomas VM, et al. Recent advancements of plant-based natural fiber–reinforced composites and their applications. Compos B Eng. 2020;200:108254.
[7] Kwon DJ, Wang ZJ, Choi JY, et al. Interfacial and mechanical properties of epoxy composites containing carbon nanotubes grafted with alkyl chains of different length. Compos Part A Appl Sci Manuf. 2016;82:190–197.
[8] Lu C, Wang J, Lu X, et al. Wettability and Interfacial properties of carbon fiber and poly (ether ether ketone) fiber hybrid composite. Appl Mater Interfaces. 2019;11 (34):31520–31531.
[9] Tian J, Xu T, Zhang Z, et al. Study on the construction of polyethyleneimine/nano-silica multilayer film on the carbon fiber surfaces to improve the interfacial properties of carbon fiber/epoxy composites. Compos Interfaces. 2022;29(4):361–381.
[10] Xu Z, Chen L, Huang Y, et al. Wettability of carbon fibers modified by acrylic acid and interface properties of carbon fiber/epoxy. Eur Polym J. 2008;44(2):494–503.
[11] Ho MP, Wnag H, Lee JH, et al. Critical factors on manufacturing processes of natural fibre composites. Compos B Eng. 2012;43(8):3549–3562.
[12] Ohnishi A, Ohori S, Funami F, et al. Improvement of resin impregnation into glass cloth by silane treatment in resin transfer molding. Compos Interfaces. 2005;12(7):683–689.
[13] Patel N, Lee LJ. Effects of fiber mat architecture on void formation and removal in liquid composite molding. Polym Compos. 1995;16(5):386–399.
[14] Mehdikhani M, Gorbatikh L, Verpoest I, et al. Voids in fiber-reinforced polymer composites: a review on their formation, characteristics, and effects on mechanical performance. J Compos Meter. 2018;53(12):1579–1669.
[15] Desai AV, Haque MA. Mechanics of the interface for carbon nanotube–polymer composites. Thin-Walled Struct. 2005;43(11):1787–1803.
[16] Sui X, Shi J, Yao H, et al. Interfacial and fatigue-resistant synergetic enhancement of carbon fiber/epoxy hierarchical composites via an electrophoresis deposited carbon nanotube-toughened transition layer. Compos Part A Appl Sci Manuf. 2017;92:134–144.
[17] Zhao J, Liebscher M, Tzounis L, et al. Role of sizing agent on the microstructure morphology and mechanical properties of mineral-impregnated carbon-fiber (MCF) reinforcement made with geopolymers. Appl Surf Sci. 2021;567:150740.
[18] Park HS, Shin PS, Kim JH, et al. Evaluation of interfacial and mechanical properties of glass fiber/poly-dicyclopentadiene composites with different post curing at ambient and low temperatures. Fibers Polym. 2018;19(9):1989–1996.
[19] Kwon DJ, Kim JH, Park SM, et al. Damage sensing, mechanical and interfacial properties of resins suitable for new CFRP rope for elevator applications. Compos B Eng. 2019;157:259–265.
[20] Lim SH, On SY, Kim H, et al. Resin impregnation and interfacial adhesion behaviors in carbon fiber/epoxy composites: effects of polymer slip and normalized surface free energy with respect to the sizing agents. Compos Part A Appl Sci Manuf. 2021;146:106424.
[21] Testoni GA, Kim SH, Pisupati A, et al. Modeling of the capillary wicking of flax fibers by considering the effects of fiber swelling and liquid absorption. J Colloid Interface Sci. 2018;525:166–176.
[22] Pucci MF, Liotier PJ, Drapier S. Permeability evaluation via wicking tests. Effect of wetting properties of test liquids. Proceedings of the 18th European Conference on Composite Materials; 2018 June 24-28; Athens, Greece.
[23] Causse P, Ravey C, Trochu F. Capillary characterization of fibrous reinforcement and optimization of injection strategy in resin transfer molding. J Compos Sci. 2018;2(2):19.

[24] Kim JH, Kwon DJ, Shin PS, et al. Interfacial properties and permeability of three patterned glass fiber/epoxy composites by VARTM. Compos B Eng. 2018;148:61–67.
[25] Mbakop RS, Lebrun G, Brouillette F. Effect of compaction parameters on preform permeability and mechanical properties of unidirectional flax fiber composites. Compos B Eng. 2019;176:107083.
[26] Seong DG, Kim JS, Um MK, et al. Investigation on the mold compressive stage of compression resin transfer molding by using in-situ measurement of permeability variation of fiber preform. Fibers Polym. 2019;20(3):651–655.
[27] Szymczyk K, Zdziennicka A, Krawczyk J, et al. Wettability, adhesion, adsorption and interface tension in the polymer/surfactant aqueous solution system: II. Work of adhesion and adsorption of surfactant at polymer–solution and solution–air interfaces. Colloids Surf A Physicochem Eng Asp. 2012; 402:139–145.
[28] Kim SH, Park SJ. Effect of graphene oxide/graphitic nanofiber nanohybrids on interfacial properties and fracture toughness of carbon fibers-reinforced epoxy matrix composites. Compos B Eng. 2021;277:109387.
[29] Kasson A, Fiddler F. Effects of surface treatment on adhesion for plastic components. Plastics Decorating. [cited 2020 May 7]. Available from: https://plasticsdecorating.com/articles/2020/effects-of-surface-treatment-on-adhesion-for-plastic-components/ .
[30] Kinloch AJ. Adhesion and adhesives: science and technology. London (UK): Chapman and Hall; 1987.
[31] Dilsiz N, Wightman JP. Effect of acid–base properties of desized and sized carbon fibers on fiber/epoxy matrix adhesion. Colloids Surf A Physicochem Eng Asp. 2000;164(2–3):325–336.
[32] Owen DK, Wendth RC. Estimation of the surface free energy of polymer. J App Polym Sci. 1969;13(8):1741–1747.
[33] Tian G, Chen B, Qi S, et al. Enhanced surface free energy of polyimide fibers by alkali treatment and its interfacial adhesion behavior to epoxy resins. Compos Interfaces. 2016;23(2):145–155.
[34] Chan Y, Sun T, Fan C, et al. The effect of surface modification on the properties of sisal fiber and improvement of interfacial adhesion in sisal/starch composites induced by starch nanocrystals. Compos Interfaces. 2018;25(11):981–994.
[35] Wang Y, Hansen CJ, McAninch IM, et al. Resin wettability correlates linearly to interfacial fracture energy between thermosetting elastomers and glass. ACS Appl Polym Mater. 2022;4(6):5244–5253.
[36] Heng JYY, Pearse DF, Thielmann F, et al. Methods to determine surface energies of natural fibres: a review. Compos Interfaces. 2007;14(7–9):581–604.
[37] Narayanamurthy V, Jeroish ZE, Bhuvaneshwari KS, et al. Advances in passively driven microfluidics and lab-on-chip devices: a comprehensive literature review and patent analysis. RSC Adv. 2020;10(20):11652–11680.
[38] Yeager M, Simacek P, Advani SG. Prediction of micro impregnation phenomena in additively manufactured composite materials. Compos Part A Appl Sci Manuf. 2022;156:106861.
[39] Washburn EW. The dynamics of capillary flow. Phys Rev. 1921;17(3):273–283.
[40] Michaud V. Composite reinforcements for optimum performance. 2nd ed. Sawston (UK): Woodhead Publishing; 2020.
[41] Yang B, Huang W, Causse P, et al. On the design of test molds based on unidirectional saturated flows to measure transverse permeability in liquid composite molding. Polym Compos. 2022;43(4):2234–2251.
[42] Ameri E, Lebrun G, Laperriere L. In-plane permeability characterization of a unidirectional flax/paper reinforcement for liquid composite molding processes. Compos Part A Appl Sci Manuf. 2016;85:52–64.
[43] Bouvard JL, Francis DK, Tschopp MA, et al. An internal state variable material model for predicting the time, thermomechanical, and stress state dependence of amorphous glassy polymers under large deformation. Int J Plast. 2013;42:168–193.

[44] Ebnesajjad S, Landrock AH. Adhesives technology handbook. London (UK): William Andrew; 2014.
[45] Lin K, Yu T. Debonding simulation of fibre-matrix interfaces of FRP composites with reactive force field. Constr Build Mater. 2021;312:125304.
[46] Kim JH, Kwon DJ, Shin PS, et al. Evaluation of interfacial and mechanical properties of glass fiber and p-DCPD composites with surface treatment of glass fiber. Compos B Eng. 2018;153:420–428.
[47] Ma Q, Gu Y, Li M, et al. Effects of surface treating methods of high-strength carbon fibers on interfacial properties of epoxy resin matrix composite. Appl Surf Sci. 2016;379:199–205.
[48] Jiao W, Hou C, Zhang X, et al. Molecular dynamics simulation of the influence of sizing agent on the interfacial properties of sized carbon fiber/vinyl ester resin composite modified by self-migration method. Compos Interfaces. 2021;28(5):445–459.
[49] Page SA, Mezzenga R, Boogh L, et al. Surface energetics evolution during processing of epoxy resins. J Colloid Interface Sci. 2000;222(1):55–62.
[50] Minisini B, Rolere S, Coulon JF, et al. Influence of the chemical composition and formulation of fluorinated epoxy resin on its surface characteristics. Eur Polym J. 2019;112:452–460.
[51] Shin PS, Baek YM, Kim JH, et al. Interfacial and wetting properties between glass fiber and epoxy resins with different pot lifes. Colloids Surf A Physicochem Eng Asp. 2018;544:68–77.
[52] Li X, Mishra K, Seul SD, et al. Microstructure and properties of poly(butylene terephthalate) based nanocomposites. Compos Interfaces. 2004;11(4):335–346.
[53] Kalin M, Polajnar M. The effect of wetting and surface energy on the friction and slip in oil-lubricated contacts. Tribol Lett. 2013;52(2):185–194.
[54] Sun G, Stark R, Kappl M, et al. Interaction between two solid surfaces across PDMS: influence of chain length and end group. Compos Interfaces. 2005;12(8–9):805–815.
[55] Lowry E, Sedghi M, Goual L. Polymers for asphaltene dispersion: interaction mechanisms and molecular design considerations. J Mol Liq. 2017;230:589–599.
[56] Vins V, Fransen M, Hykl J, et al. Surface tension of supercooled water determined by using a counterpressure capillary rise method. J Phys Chem B. 2015;119(17):5567–5575.
[57] Yeaher M, Hang WR, Advani SG. Prediction of capillary pressure for resin flow between fibers. Compos Sci Technol. 2016;126:130–138.
[58] Zheng Z, Wang X, Huang X, et al. Wetting behavior of modified vinylester resins on the surface of UHMWPE materials. Compos Interfaces. 2008;15(1):35–48.
[59] Caglar B, Tekin C, Karasu F, et al. Assessment of capillary phenomena in liquid composite molding. Compos Part A Appl Sci Manuf. 2019;120:73–83.
[60] Vo HN, Pucci MF, Drapier S, et al. Capillary pressure contribution in fabrics as a function of fibre volume fraction for liquid composite moulding processes. Colloids Surf A Physicochem Eng Asp. 2022;635:128120.
[61] Abdulmajeed AA, Narhi TO, Vallittu PK, et al. The effect of high fiber fraction on some mechanical properties of unidirectional glass fiber-reinforced composite. Dent Mater. 2011;27(4):313–321.
[62] Hassanzadeh-Aghdam MK, Mahnoodi MJ, Ansari R. Micromechanics-based characterization of mechanical properties of fuzzy fiber-reinforced composites containing carbon nanotubes. Mech Mater. 2018;118:31–43.
[63] Lee DH, Lee WI, Kang MK. Analysis and minimization of void formation during resin transfer molding process. Compos Sci Technol. 2006;66(16):3281–3289.
[64] Lu X, Tsotsas E, Kharaghani A. Drying of capillary porous media simulated by coupling of continuum-scale and micro-scale models. Int J Multiphase Flow. 2021;140:103654.
[65] Shi B, Shang Y, Zhang P, et al. Dynamic capillary-driven additive manufacturing of continuous carbon fiber composite. Matter. 2020;2(6):1594–1604.
[66] Domanska U, Zawadzki M, Lewandrowska A. Effect of temperature and composition on the density, viscosity, surface tension, and thermodynamic properties of binary mixtures of N-octylisoquinolinium bis{(trifluoromethyl)sulfonyl}imide with alcohols. J Chem Thermodyn. 2012;48:101–111.

[67] Zhang S, Zhao L, Yue X, et al. Density, viscosity, surface tension and spectroscopic studies for the liquid mixture of tetraethylene glycol + N,N-dimethylformamide at six temperatures. J Mol Liq. 2018;264:451–457.
[68] Yuan X, Zhu B, Cai X, et al. Influence of different surface treatments on the interfacial adhesion of graphene oxide/carbon fiber/epoxy composites. Appl Surf Sci. 2018;458:996–1005.
[69] Sharma M, Gao S, Mader E, et al. Carbon fiber surfaces and composite interphases. Compos Sci Technol. 2014;102:35–50.
[70] Shin PS, Kim JH, Park HS, et al. Advanced interfacial properties of glass fiber/dopamine-epoxy composites using a microdroplet pull-out test and acoustic emission. J Adhes. 2021;97 (5):438–455.
[71] Schechter SGK, Centea T, Nutt SR. Polymer film dewetting for fabrication of out-of-autoclave prepreg with high through-thickness permeability. Compos Part A Appl Sci Manuf. 2018;114:86–96.
[72] Naresh K, Khan KA, Cantwell WJ. The use of X-ray computed tomography for design and process modeling of aerospace composites: a review. Mater Des. 2020;190:108553.
[73] Liu DSC, Hubert P. Bulk factor characterization of heated debulked autoclave and out-of-autoclave carbon fibre prepregs. Compos B Eng. 2021;219:108940.
[74] Alotaibi H, Jabbari M, Abeykoon C, et al. Numerical investigation of multi-scale characteristics of single and multi-layered woven structures. Appl Compos Mater. 2022;29 (1):405–421.
[75] Sadeghian R, Gangireddy S, Minaie B, et al. Manufacturing carbon nanofibers toughened polyester/glass fiber composites using vacuum assisted resin transfer molding for enhancing the mode-I delamination resistance. Compos Part A Appl Sci Manuf. 2006;37 (10):1787–1795.
[76] Wang S, Haldane D, Liang R, et al. Nanoscale infiltration behaviour and through-thickness permeability of carbon nanotube buckypapers. Nanotechnol. 2013;24(1):015704.
[77] Poppe C, Dorr D, Henning F, et al. Experimental and numerical investigation of the shear behaviour of infiltrated woven fabrics. Compos A Appl Sci Manf. 2018; 114:327–337.
[78] Kim DJ, Yu MH, Lim JY, et al. Prediction of the mechanical behavior of fiber-reinforced composite structure considering its shear angle distribution generated during thermo-compression molding process. Compos Struct. 2019;220:441–450.
[79] Perez-de-eulate NG, Ortega N, Holgado I, et al. The effect of preforming and infusing bindered and unbindered carbon non-crimp-fabrics on the final quality of composites parts. J Mater Res Technol. 2022;17:2725–2741.
[80] Heardman E, Lekakou C, Bader MG. In-plane permeability of sheared fabrics. Compos Part A Appl Sci Manuf. 2001;32(7):933–940.
[81] Marar K, Eren O, Roughani H. The influence of amount and aspect ratio of fibers on shear behaviour of steel fiber reinforced concrete. KSCE J Civ Eng. 2017;21(4):1393–1399.
[82] Kim JI, Hwang YT, Choi KH, et al. Prediction of the vacuum assisted resin transfer molding (VARTM) process considering the directional permeability of sheared woven fabric. Compos Struct. 2019;211:236–243.
[83] Potluri P, Perez Ciurezu DA, Ramgulam RB. Measurement of meso-scale shear deformations for modelling textile composites. Compos Part A Appl Sci Manuf. 2006;37(2):303–314.
[84] Cao J, Akkerman R, Boisse P, et al. Characterization of mechanical behavior of woven fabrics: experimental methods and benchmark results. Compos Part A Appl Sci Manuf. 2008;39(6):1037–1053.